Extremely Low Electron-ion Temperature Relaxation Rates in Warm Dense Hydrogen: Interplay between Quantum Electrons and Coupled Ions

Qian Ma,[1] Jiayu Dai,[1,*] Dongdong Kang,[1] M. S. Murillo,[2] Yong Hou,[1] Zengxiu Zhao,[1,†] and Jianmin Yuan[1,3]
[1]Department of Physics, National University of Defense Technology, Changsha, Hunan 410073, P. R. China
[2]Department of Computational Mathematics, Science and Engineering, Michigan State University, East Lansing, Michigan 48824, USA
[3]Graduate School of China Academy of Engineering Physics, Beijing 100193, P. R. China

(Received 2 March 2017; revised manuscript received 24 October 2018; published 8 January 2019)

Theoretical and computational modeling of nonequilibrium processes in warm dense matter represents a significant challenge. The electron-ion relaxation process in warm dense hydrogen is investigated here by nonequilibrium molecular dynamics using the constrained electron force field (CEFF) method. CEFF evolves wave packets that incorporate dynamic quantum diffraction that obviates the Coulomb catastrophe. Predictions from this model reveal temperature relaxation times as much as three times longer than prior molecular dynamics results based on quantum statistical potentials. Through analyses of energy distributions and mean free paths, this result can be traced to delocalization. Finally, an improved GMS [Gericke, Murillo, and Schlanges, Phys. Rev. E **78**, 025401 (2008)] model is proposed, in which the Coulomb logarithms are in good agreement with CEFF results.

DOI: 10.1103/PhysRevLett.122.015001

Warm dense matter (WDM) is commonly defined as matter with both partially degenerate electrons and strongly coupled ions, a state of matter that introduces challenges both experimentally and theoretically. These challenges are exacerbated in studies of nonequilibrium processes, such as electron-ion energy exchange processes that occur within laser-matter interactions such as inertial-confinement fusion [1–3]. The emergence of large laser facilities, such as the National Ignition Facility and the Linac Coherent Light Source, allows us to create and probe WDM with increasing ease [4–6]; however, diagnosing WDM remains a challenge. X-ray Thomson scattering techniques allow the measurement of evolving temperatures [7–9], which indicates that the ion-electron energy exchange rate is much lower than the current theoretical models and classical molecular dynamics (CMD) simulations predict [10–14]. Xu and Hu have shown the sensitivity to relaxation rates on laser energy depositions [2], motivating us to obtain more accurate rates.

The process of temperature relaxation in WDM is a probe of electron-ion collisions in a complex state of matter. In particular, this process probes nonadiabatic dynamics in the presence of dynamical many-body correlations. Landau and Spitzer (LS) theory [15,16] can be derived from a Fokker-Planck equation, which is appropriate for dilute, weakly coupled plasmas. The LS electron-ion temperature relaxation rate ($\nu_{\rm ei}$) is given by

$$\nu_{\rm ei} = \frac{8\sqrt{2\pi}n_i Z^2 e^4}{3mM}\left(\frac{k_B T_e}{m}+\frac{k_B T_i}{M}\right)^{-3/2}\ln\Lambda, \qquad (1)$$

where $m(M)$, $e(Ze)$, and $n_e(n_i)$ are the mass, charge, density of the electrons (ions), respectively, and k_B is the Boltzmann constant. Here, $\ln\Lambda$ is the Coulomb logarithm, which is typically characterized as $\ln(b_{\rm max}/b_{\rm min})$, with $b_{\rm max}$ ($b_{\rm min}$) being the maximum (minimum) impact parameter. The impact parameters $b_{\rm max}$ and $b_{\rm min}$ are chosen by considerations external to the LS theory; typically, $b_{\rm max}$ is treated as the electron Debye length $\lambda_D = \sqrt{k_B T_e/4\pi n_e e^2}$, and $b_{\rm min}$ is chosen as either the classical distance of closest approach ($b_0 = Ze^2/k_B T_e$) or the electron thermal de Broglie wavelength $\Lambda_0 = \hbar\sqrt{2\pi/m_e k_B T_e}$. Extensions that include many-body corrections, such as the Fermi golden rule [17,18], Lenard-Balescu [19–21], and coupled models [18,22,23], have been developed using linear response relations. A convergent kinetic theory was developed by Brown, Preston, and Singleton (BPS) [24] using a dimensional continuation method without any *ad hoc* cutoff. Gericke, Murillo, and Schlanges (GMS) [25] introduced an effective screening length that incorporates strong coupling and large-angle scattering. These models have been validated for nondegenerate plasmas; however, extensions of these models in nonequilibrium WDM are questionable because of the coupling between quantum dynamics and modes of strongly coupled ions.

Molecular dynamics (MD) simulation is a powerful method for investigating temperature relaxation in strongly coupled plasmas [26–36] because it includes self-consistent collective modes with arbitrary-angle scattering without *ad hoc* cutoffs. This level of accuracy, however, is the

source of the Coulomb catastrophe in CMD in which deeply bound pairs of electrons and ions can form. In practice, this is mitigated through the use of, for example, quantum statistical potentials (QSP) [26–28,37,38]. Alternatively, an electronic structure method, such as density functional theory, can be employed to study the properties of warm dense matter [39–42]; however, by capitalizing on the Born-Oppenheimer approximation, such methods neglect electron dynamics. Improvements are possible through time-dependent density functional theory, which is currently extremely expensive and has questionable fidelity in modeling fluctuating kinetic phenomena [43]. Thus, a more accurate and efficient method is needed to design and describe nonadiabatic dynamics in WDM environments.

Here, we improved the electron force field (EFF) method and applied it to electron-ion temperature relaxation in warm dense hydrogen. The EFF method is an extension of wave packet molecular dynamics (WPMD), which has been successfully used to describe the structure and properties of complex systems, such as the thermodynamics of shock-compressed hydrogen, Auger processes in diamondoids and the equation of state for lithium [44–49]. The basis of the EFF method is the variational solution of the time-dependent Schrödinger equation subject to a Gaussian wave packet ansatz. The ions remain classical point charges, with nuclear quantum effects neglected. With only a few new degrees of freedom, it is practical to use the EFF method to model the nonequilibrium dynamics of large-scale quantum systems, including quantum degeneracy, tunneling, dissociation, and excitation, ionization, or recombination. The electronic radial vibration in the wave packets describes the hopping of electrons between different states at different times [50].

However, WPMD or EFF models are not without their limitations, with the main concern being the well-known wave packet spreading at high temperatures [51]. Although we anticipate that collective effects and large-angle collisions in warm dense matter will reduce this spreading significantly, [50,52] we quantify and calibrate our EFF method accordingly. Historically, wave packet spreading has been avoided through harmonic constraints [53] and periodic boundary conditions for the width coordinate [52]. Here, we use $L = \lambda_D + b_0$ as the boundary of the wave packets. Within this framework of constrained EFF (CEFF), the width dispersion of wave packets can be constrained well. Moreover, we redefine the electron temperature as $(F_{\mathrm{dof}}/2)N_e k_B T_e = \sum_i (\frac{1}{2} m_e \mathbf{v}_i^2 + \frac{1}{2}\frac{3}{4} m_e \dot{s}_i^2)$, in which F_{dof} is the freedom of electron, and it is 4 here considering electronic radial vibration and translational motion. T_e and N_e are the electronic temperature and number, and $\mathbf{v}_i$ and $\dot{s}_i$ are translational velocities of the electrons and the radial vibrational velocities, respectively.

In order to validate our CEFF models, we plotted the distribution of the radii of wave packets in the dynamics of temperature relaxation, as shown in Fig. 1. In previous

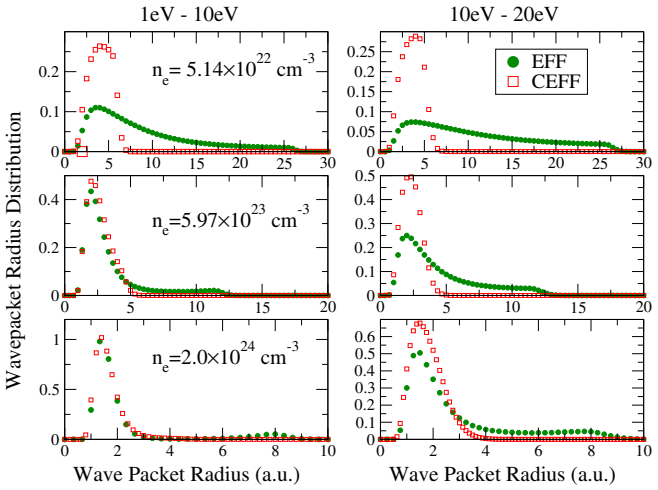

FIG. 1. The radius of wave packets of the temperature relaxation of warm dense hydrogen with initial electronic temperature $T_{e0} = 10$ eV and ionic temperature $T_{i0} = 1$ eV (left column), $T_{e0} = 20$ eV and $T_{i0} = 10$ eV (right column) with different densities n_e. Green dotted lines represent the radii from original EFF using boundary of half box size, red square lines are our CEFF results.

studies, using half the size of the supercell as the maximum wave packet width, EFF has been shown to be a valid approach. At high temperature, the electrons should become more localized, but we can see that at low density, the wave packets spread to the entire box. However, the wave packets can be kept localized with CEFF, indicating that nonphysical dispersion can be avoided. Moreover, the middle peak of the wave packets corresponds to a de Broglie wavelength of 4.7 a.u.. When the density increases, the difference between EFF and CEFF become small, which means that the choice of boundary for high-density systems is not important. This conclusion can promise the validation of our EFF and CEFF for warm dense hydrogen at relatively high densities. [50].

We now turn to relaxation comparisons between CEFF and QSP models, as implemented in the LAMMPS [47] package. The electron number densities range from 5.1×10^{22} cm^{-3} to 6.0×10^{24} cm^{-3}, the initial electronic temperature T_{e0} is varied from 10 eV to 20 eV, and the initial ionic temperature T_{i0} is varied from 1 eV to 10 eV. The corresponding ionic coupling parameter $\Gamma_{\mathrm{ii}} = Z^{*2}/(r_i k_B T)$, where Z^* is the ionization degree of ions, $r_i = [3/(4\pi n_i)]^{1/3}$, can be as large as 42, the electron degeneracy parameter $\Theta = T/T_F$, the Fermi temperature $T_F = (3\pi^2 n_e)^{2/3}/2$, can take on values up to 0.08.

We equilibrate the ion and electron subsystems with isokinetic thermostats at separate temperatures to generate two-temperature initial conditions. The thermostat is released to relax the system in the microcanonical ensemble. The time step ranged from 10^{-3} fs to 2.0×10^{-4} fs. Convergence with respect to particle number was examined,

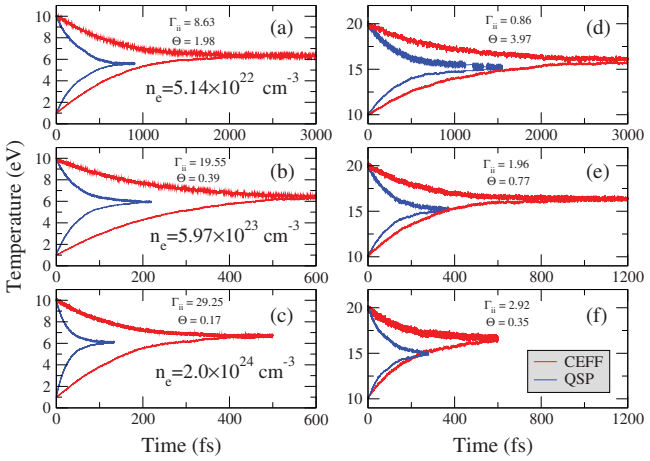

FIG. 2. The temporal evolution of ionic and electronic temperatures at different densities. The initial electronic temperature $T_{e0} = 10$ eV and ionic temperature $T_{i0} = 1$ eV [(d)–(f)], $T_{e0} = 20$ eV and $T_{i0} = 10$ eV [(a)–(c)]. The red curves are results from the CEFF method while the blue curves are from CMD with QSP. The related parameters are $\Gamma_{ii} = 8.63, 19.55, 29.25, 0.86, 1.96, 2.92$ and $\Theta = 1.98, 0.39, 0.17, 3.97, 0.77, 0.35$ corresponding to the initial temperature, respectively.

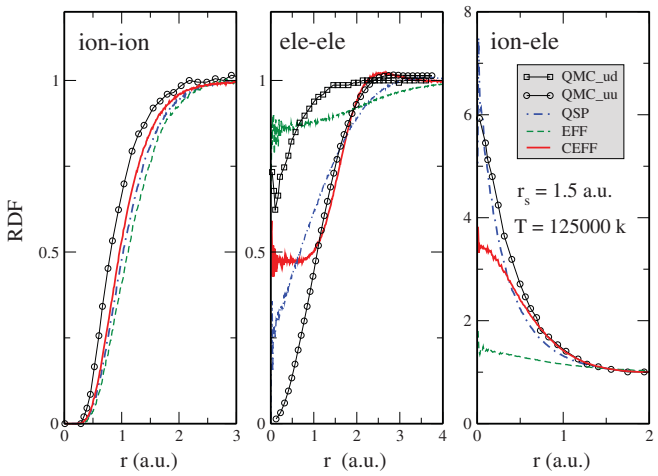

FIG. 3. RDFs calculated from EFF, CEFF, CMD with QSP, and PIMC in equilibrium conditions. Here, the temperature is 125 000 K and the Wigner radius is 1.5 Bohr. The ion-ion (ii) distribution g_{ii}, electron-electron (ee) distribution g_{ee}, and ion-electron (ie) distribution g_{ie} are shown. For PIMC, the spin-resolved RDFs are shown.

and $N_e = N_i = 1000$ was adopted [50]. Statistical fluctuations are accounted for by averaging 10 initial configurations. The physical masses of electrons and ions were used.

In Fig. 2, the temporal evolutions of ionic and electronic temperature in different densities are shown. It is shown that the ion-electron relaxation times in CEFF are considerably longer than those from CMD with QSP. In Fig. 2(a), the relaxation time in CEFF is about 2040 fs, while in CMD, the time is about 750 fs. Furthermore, we find that the final equilibrium temperature in CEFF is higher than that in CMD. In CMD, electrons and ions are both classical particles, with kinetic energies of $3/2k_BT$. In Fig. 2(d), the final equilibrium temperature in EFF is about 5.8% higher than that in CMD, 8.5% higher in Fig. 2(e), and 10.2% higher in Fig. 2(f). The thermal capacity of quantum electrons is larger than that of classical electrons, as can be seen in Fig. 2 in the Supplemental Material [50]. When the density is higher, quantum degeneracy effects should be more significant, inducing larger kinetic energies of electrons.

To provide a deeper understanding of the discrepancy between CEFF and QSP models for relaxation, we performed further comparisons with quantum Monte Carlo calculations [54,55]. In Fig. 3, the radial distribution functions (RDFs) of ion-ion (g_{ii}), electron-electron (g_{ee}), and ion-electron (g_{ie}) from EFF, CEFF, CMD (QSP), and path integral Monte Carlo calculations (PIMC) are shown. Compared with PIMC simulations [54], we see that the g_{ii} of CEFF is improved relative to the other models; in particular, the EFF tends to underestimate ion-ion correlations. For g_{ee}, since CEFF and EFF give the RDFs without spin resolution, it is also shown that EFF gives more delocalized electronic distributions, although the spin-averaged PIMC result is similar to the CEFF result. More interesting is g_{ie}: the g_{ie} of QSP and PIMC agree well with each other, with QSP giving higher values than CEFF near zero distance. Moreover, the g_{ie} of CEFF is lower than that of PIMC near zero separation, indicating the coupling of electrons and ions in CEFF is weaker than that of PIMC and QSP. We should note that in the present PIMC, plane wave (PW) nodes were used, and the variational density matrix (VDM) method, which is more accurate, gives lower electron-ion distributions [54]. Perhaps this is because the electrons with high momentum near the nucleus cannot be described well in PIMC with PW nodes. This means that, in PIMC and QSP, the interactions between electrons and ions are overestimated significantly, which will obviously introduce faster equilibrium dynamics for temperature relaxations. In WPMD, it shows that for some quantities exponentials can be better than Gaussians [56], and this might be why the correct cusp condition in the figure with g_{ie} is too soft with Gaussians, indicating that CEFF can be further improved. Moreover, CMD with QSPs can be a good choice for statistical quantities for moderately degenerate systems, but this method fails for strong degeneracy. [57] In EFF and CEFF, the sizes of electronic wave packets are time dependent, and all the energies and dynamics are dependent on the widths, which are not included in CMD. In addition, EFF with a free boundary will give nonphysical, smaller relaxation rates since the interactions between ions and electrons are so weak at lower densities, because the wave packets will be too dispersed. At high densities, the relaxation dynamics should be in agreement with CEFF, as shown in Fig. 1.

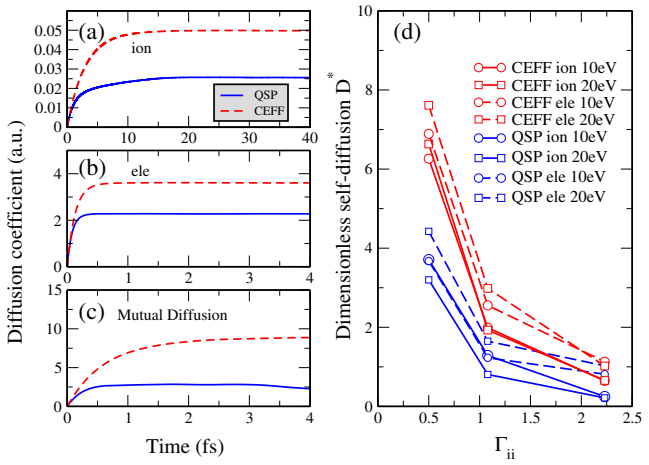

FIG. 4. The diffusion coefficients D [(a),(b), and (c)] are at the electron number density of 2.0×10^{24} cm^{-3} and the temperature of 20 eV. The dimensionless self-diffusion coefficients D^* versus Γ_{ii} are shown in (d), in which data points indicated with circles are at 10 eV, and data points indicated with squares are at 20 eV.

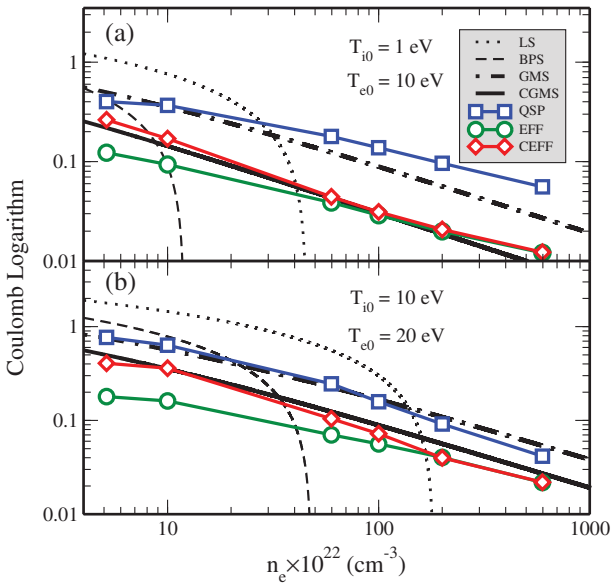

FIG. 5. Coulomb logarithm calculated from theoretical methods [LS (black dotted), BPS (black dashed), GMS (black dotted dash line), coupled GMS (CGMS, black solid line)] and molecular dynamics simulations [CMD (blue square), EFF (green circle), and CEFF (red diamond)]. Initial temperatures are $T_{e0} = 10$ eV and $T_{i0} = 1$ eV in (a), $T_{e0} = 20$ eV and $T_{i0} = 10$ eV in (b). Electron number density is chosen from $n_e = 5.1 \times 10^{22}$ cm^{-3} to $n_e = 6.0 \times 10^{24}$ cm^{-3}.

The energy exchange rate is dependent on the scattering cross section or mean free path (MFP) of the particles. We show a comparison of self-diffusion and the mutual diffusion coefficient in an equilibrium state between CEFF and CMD in Figs. 4(a), 4(b), and 4(c). The self-diffusion and mutual coefficients D can be calculated using the Green-Kubo relation [50,58–60]. It can be shown that the diffusion coefficients calculated from CEFF are larger than those from CMD.

We estimate the MFP of the particles using $D = \bar{v}\,\bar{r}\,/3$ [61], where $\bar{v}$ is the average velocity, and $\bar{r}$ is the MFP. Here, in CEFF, the MFPs are 8.02 a.u. for electrons and 4.6 a.u. for ions, while in CMD, the MFP are 5.0 a.u. for electrons and 2.4 a.u. for ions. This indicates that electronic quantum effects allow ions or electrons to travel more easily in warm dense hydrogen. The MFP is inversely proportional to the scattering cross section, which is smaller for quantum particles than that for classical particles. In particular, the mutual diffusion of CEFF is more than three times larger than that of CMD, indicating the cross section between electrons and ions is much lower in CEFF. In warm dense matter, these large-angle collisions dominate the energy exchange rates, so that the relaxation time is much lower within the framework of CEFF.

To understand the interplay between quantum electrons and coupled ions, the dimensionless self-diffusion coefficient $D^* = D/\omega_i r_i^2$ [21] versus Γ_{ii} is shown in Fig. 4(d), where $\omega_i = (4\pi n_i Z^2 e^2/m_i)^{1/2}$ is the plasma frequency and $r_i = [3/(4\pi n_i)]^{1/3}$. As the dimensionless self-diffusion D^* is normalized by the mass of the corresponding species, the difference in D^* between ions and electrons can reveal the quantum effects of electrons. We find that the D^* of electrons and ions in CMD are similar since ions and electrons are both classical charged points. However, in CEFF, the D^* of electrons is larger than that of ions. Furthermore, the D^* from CEFF is larger than that from CMD, which is caused by the interactions between quantum electrons and coupled ions. When Γ_{ii} increases with a fixed temperature, the electrons become more localized [50], so that the difference in D^* between ions and electrons in CEFF becomes smaller.

Since kinetic models give faster dynamics compared with experiments and CEFF results, how can we improve these models? Coulomb logarithms can be derived using different methods and are important inputs into hydrodynamic modeling codes [2]. The temperature relaxation rates of electrons and ions can be written as $dT_e/dt = -\nu_{ei}(T_e - T_i)$ and $dT_i/dt = -\nu_{ie}(T_i - T_e)$, respectively. Here, we assume $\nu_{ei} = \nu_{ie}$, as the deviation is small in most cases. The average temperature relaxation rate ν_{ei} can be calculated by fitting the formula $d\Delta T/dt = -2\nu_{ei}\Delta T$, where $\Delta T = T_e - T_i$ is obtained from simulation results. The Coulomb logarithms are then derived based on Eq. (1). In the GMS model, the Coulomb logarithm can be written as $L_{GMS} = \frac{1}{2}\ln\{1 + [(\lambda_D^2 + R_i^2)/(\Lambda^2/8\pi + b_c^2)]\}$ [62], where R_i is the ionic distance, and typically $b_c = b_0 = Ze^2/k_B T_e$, which only considers the electron interactions. Here, we propose to introduce the coupling between electrons and ions, defining $b_c = \frac{1}{2}Ze^2/(k_B T_e + k_B T_i)$. In this coupled GMS (CGMS) model, we can obtain a new form of the Coulomb logarithm that includes dynamical electron-ion

coupling. Figure 5 shows that the Coulomb logarithm $\ln\Lambda$ increases as the electron temperature increases, but decreases as the electron number density increases under the conditions studied here. It is shown that EFF and CEFF give much lower Coulomb logarithms; they differ at low densities, but become consistent at high densities ($n_e = 2.0 \times 10^{24}$ cm^{-3}). Importantly, the CGMS model agrees well with CEFF across all regimes explored in this Letter, revealing the importance of electron-ion coupling in WDM.

We estimate the computational errors in the simulated results to be between 1% and 13%. The remarkable effects introduced by the quantum effects of electronic degeneracy, delocalization, and quantum collisions should be natural in warm dense matter, and these effects could substantially change the energy deposition processes in laser-matter interactions. Recent direct experiments measuring the temperature-relaxation dynamics in LCLS indicate that the dynamics in warm dense hydrogen is really much slower than those predicted previously using theoretical models [63].

In summary, we have developed the constrained EFF method to study the temperature relaxation of warm dense hydrogen. The energy exchange rates are much slower than those predicted by previous models. Wave packet dynamics induce a much larger mean free path for large-angle collisions, and quantum electron dynamics dominated WDM. Results of the coupled GMS model, which introduces coupling between ions and electrons, are in good agreement with constrained EFF results, which gives us information that will help us to improve kinetic models in the future. This Letter will allow an improved understanding of laser-matter interactions at the microscopic level, additional validations of theoretical models, and a greater understanding of the hydrodynamics of laser-matter interactions. The present method can also be implemented to study electron dynamics-related physics such as x-ray Thomson scattering spectra and stopping power.

This Letter was supported by the Science Challenge Project under Grant No. TZ2016001, the National NSFC under Grants No. 11774429, 11874424, and U1830206, the National Key R&D Program of China under Grant No. 2017YFA0403200, the Science and Technology Project of Hunan Province under Grant No. 2017RS3038, and the Advanced Research Foundation of the National University of Defense Technology under Grant No. JQ14-02-01. Calculations were carried out at the Research Center of Supercomputing Applications at NUDT.

*Corresponding author.
jydai@nudt.edu.cn
†zhaozengxiu@nudt.edu.cn

[1] S. Atzeni and J. Meyer-ter-Vehn, *The Physics of Inertial Fusion* (Clarendon Press, Oxford, 2004).
[2] B. Xu and S. X. Hu, Phys. Rev. E **84**, 016408 (2011).
[3] S. H. Glenzer *et al.*, Science **327**, 1228 (2010).
[4] V. N. Goncharov *et al.*, Phys. Rev. Lett. **104**, 165001 (2010).
[5] A. Ng, Int. J. Quantum Chem. **112**, 150 (2012).
[6] P. Celliers, A. Ng, G. Xu, and A. Forsman, Phys. Rev. Lett. **68**, 2305 (1992).
[7] L. B. Fletcher *et al.*, Nat. Photonics **9**, 274 (2015).
[8] S. H. Glenzer *et al.*, J. Phys. B **49**, 092001 (2016).
[9] C. Bostedt, S. Boutet, D. M. Fritz, Z. Huang, H. J. Lee, H. T. Lemke, A. Robert, W. F. Schlotter, J. J. Turner, and G. J. Williams, Rev. Mod. Phys. **88**, 015007 (2016).
[10] A. Ng, P. Celliers, G. Xu, and A. Forsman, Phys. Rev. E **52**, 4299 (1995).
[11] D. Riley, N. C. Woolsey, D. McSherry, I. Weaver, A. Djaoui, and E. Nardi, Phys. Rev. Lett. **84**, 1704 (2000).
[12] B. I. Cho *et al.*, Phys. Rev. Lett. **106**, 167601 (2011).
[13] T. G. White *et al.*, Sci. Rep. **2**, 889 (2012).
[14] T. G. White, S. Richardson, B. J. B. Crowley, L. K. Pattison, J. W. O. Harris, and G. Gregori, Phys. Rev. Lett. **111**, 175002 (2013).
[15] L. D. Landau, Zh. Eksp. Teor. Fiz. **7**, 203 (1937); Phys. Z. Sowjetunion **10**, 154 (1936).
[16] L. Spitzer, *Physics of Fully Ionized* (Interscience, New York, 1967).
[17] G. Hazak, Z. Zinamon, Y. Rosenfeld, and M. W. C. Dharma-wardana, Phys. Rev. E **64**, 066411 (2001).
[18] M. W. C. Dharma-wardana and F. Perrot, Phys. Rev. E **58**, 3705 (1998).
[19] A. Lenard, Ann. Phys. (N.Y.) **10**, 390 (1960).
[20] R. Balescu, Phys. Fluids **3**, 52 (1960).
[21] L. G. Stanton and M. S. Murillo, Phys. Rev. E **93**, 043203 (2016).
[22] D. A. Chapman, J. Vorberger, and D. O. Gericke, Phys. Rev. E **88**, 013102 (2013).
[23] L. X. Benedict *et al.*, Phys. Rev. E **95**, 043202 (2017).
[24] L. S. Brown, D. L. Preston, and R. L. Singleton, Phys. Rev. E **86**, 016406 (2012).
[25] D. O. Gericke, M. S. Murillo, and M. Schlanges, Phys. Rev. E **65**, 036418 (2002).
[26] J. P. Hansen and I. R. McDonald, Phys. Lett. **97A**, 42 (1983).
[27] J. N. Glosli, F. R. Graziani, R. M. More, M. S. Murillo, F. H. Streitz, M. P. Surh, L. X. Benedict, S. Hau-Riege, A. B. Langdon, and R. A. London, Phys. Rev. E **78**, 025401(R) (2008).
[28] M. W. C. Dharma-wardana, Phys. Rev. Lett. **101**, 035002 (2008).
[29] G. Dimonte and J. Daligault, Phys. Rev. Lett. **101**, 135001 (2008).
[30] B. Jeon, M. Foster, J. Colgan, G. Csanak, J. D. Kress, L. A. Collins, and N. Grønbech-Jensen, Phys. Rev. E **78**, 036403 (2008).
[31] L. X. Benedict, J. N. Glosli, D. F. Richards, F. H. Streitz, S. P. Hau-Riege, R. A. London, F. R. Graziani, M. S. Murillo, and J. F. Benage, Phys. Rev. Lett. **102**, 205004 (2009).
[32] F. R. Graziani *et al.*, High Energy Density Phys. **8**, 105 (2012).
[33] L. X. Benedict *et al.*, Phys. Rev. E **86**, 046406 (2012).

[34] C. Blancard, J. Clerouin, and G. Faussurier, High Energy Density Phys. **9**, 247 (2013).
[35] J. Vorberger and D. O. Gericke, High Energy Density Phys. **10**, 1 (2014).
[36] Q. Ma, J. Dai, D. Kang, Z. Zhao, J. Yuan, and X. Zhao, High Energy Density Phys. **13**, 34 (2014).
[37] H. Minoo, M. M. Gombert, and C. Deutsch, Phys. Rev. A **23**, 924 (1981).
[38] B. Bernu, J. P. Hansen, and R. Mazighi, Phys. Lett. **100A**, 28 (1984).
[39] L. Collins, I. Kwon, J. Kress, N. Troullier, and D. Lynch, Phys. Rev. E **52**, 6202 (1995); M. P. Desjarlais, J. D. Kress, and L. A. Collins, Phys. Rev. E **66**, 025401(R) (2002); S. Mazevet, M. P. Desjarlais, L. A. Collins, J. D. Kress, and N. H. Magee, Phys. Rev. E **71**, 016409 (2005).
[40] B. Holst, M. French, and R. Redmer, Phys. Rev. B **83**, 235120 (2011).
[41] J. Dai, Y. Hou, and J. Yuan, Phys. Rev. Lett. **104**, 245001 (2010); J. Dai, D. Kang, Z. Zhao, Y. Wu, and J. Yuan, Phys. Rev. Lett. **109**, 175701 (2012).
[42] S. X. Hu, B. Militzer, V. N. Goncharov, and S. Skupsky, Phys. Rev. Lett. **104**, 235003 (2010).
[43] M. Lindenblatt and E. Pehlke, Phys. Rev. Lett. **97**, 216101 (2006).
[44] J. T. Su and W. A. Goddard, III, Phys. Rev. Lett. **99**, 185003 (2007).
[45] J. T. Su and W. A. Goddard, III, Proc. Natl. Acad. Sci. U.S.A. **106**, 1001 (2009).
[46] J. T. Su and W. A. Goddard, III, J. Chem. Phys. **131**, 244501 (2009).
[47] A. Jaramillo-Botero, J. T. Su, A. Qi, and W. A. Goddard, III, J. Comput. Chem. **32**, 497 (2011).
[48] H. Kim, J. T. Su, and W. A. Goddard, III, Proc. Natl. Acad. Sci. U.S.A. **108**, 15101 (2011).
[49] P. L. Theofanis, A. Jaramillo-Botero, W. A. Goddard, III, and H. Xiao, Phys. Rev. Lett. **108**, 045501 (2012).
[50] See Supplemental Material at http://link.aps.org/supplemental/10.1103/PhysRevLett.122.015001 for detailed information about the validation of our method, and the information of kinetic and potential energies, Pauli interactions, equation for the calculations of diffusions, RDFs, and related discussions.
[51] P. E. Grabowski, A. Markmann, I. V. Morozov, I. A. Valuev, C. A. Fichtl, D. F. Richards, V. S. Batista, F. R. Graziani, and M. S. Murillo, Phys. Rev. E **87**, 063104 (2013).
[52] I. V. Morozov and I. A. Valuev, J. Phys. A **42**, 214044 (2009).
[53] M. Knaup, P. G. Reinhard, and C. Toepffer, Contrib. Plasma Phys. **39**, 57 (1999).
[54] B. Militzer and D. M. Ceperley, Phys. Rev. Lett. **85**, 1890 (2000); B. Militzer, Ph. D. thesis, University of Illinois at Urbana-Champaigne, 2000 (unpublished), see http://militzer.gl.ciw.edu/diss/diss_militzer.pdf.
[55] T. Dornheim, S. Groth, T. Schoof, C. Hann, and M. Bonitz, Phys. Rev. B **93**, 205134 (2016).
[56] M. S. Murillo and E. Timmermans, Contrib. Plasma Phys. **43**, 333 (2003).
[57] A. Diaw and M. S. Murillo, Sci. Rep. **7**, 15352 (2017).
[58] M. P. Allen and D. J. Tildesley, *Molecular Simulation of Liquids* (Oxford Science Publications, Oxford, 1987).
[59] J. Dai, Y. Hou, D. Kang, H. Sun, J. Wu, and J. Yuan, New J. Phys. **15**, 045003 (2013).
[60] Y. Hou, J. Dai, D. Kang, W. Ma, and J. Yuan, Phys. Plasmas **22**, 022711 (2015).
[61] F. Reif, *Statistical Physics: Berkeley Physics Course-Volume 5* (McGraw-Hill Book Company, New York, 1967).
[62] In this Letter, the GMS model is implicit for GMS6 in Ref. [25].
[63] L. Fletcher, *Abstract: TI2.00005, 58th Annual Meeting of the APS Division of Plasma Physics* (San Jose, California, 2016).